
M2MKD: MODULE-TO-MODULE KNOWLEDGE DISTILLATION FOR MODULAR TRANSFORMERS

¹Ka Man Lo ^{*}, ²Yiming Liang ^{*}, ³Wenyu Du, ⁴Yuantao Fan,
⁵Zili Wang, ⁶Wenhao Huang, ⁷Lei Ma [†], ⁸Jie Fu [†]

¹ University of Macau ² Institute of Automation, Chinese Academy of Sciences ³ University of Hong Kong

⁴ School of Artificial Intelligence, Beijing University of Posts and Telecommunications

⁵ Independent ⁶ 01.AI ⁷ Peking University ⁸ Hong Kong University of Science and Technology

ABSTRACT

Modular neural architectures are gaining increasing attention due to their powerful capability for generalization and sample-efficient adaptation to new domains. However, training modular models, particularly in the early stages, poses challenges due to the optimization difficulties arising from their intrinsic sparse connectivity. Leveraging the knowledge from monolithic models, using techniques such as knowledge distillation, is likely to facilitate the training of modular models and enable them to integrate knowledge from multiple models pretrained on diverse sources. Nevertheless, conventional knowledge distillation approaches are not tailored to modular models and can fail when directly applied due to the unique architectures and the enormous number of parameters involved. Motivated by these challenges, we propose a general module-to-module knowledge distillation (m2mKD) method for transferring knowledge between modules. Our approach involves teacher modules split from a pretrained monolithic model, and student modules of a modular model. m2mKD separately combines these modules with a shared meta model and encourages the student module to mimic the behaviour of the teacher module. We evaluate the effectiveness of m2mKD on two distinct modular neural architectures: Neural Attentive Circuits (NACs) and Vision Mixture-of-Experts (V-MoE). By applying m2mKD to NACs, we achieve significant improvements in IID accuracy on Tiny-ImageNet (up to 5.6%) and OOD robustness on Tiny-ImageNet-R (up to 4.2%). On average, we observe a 1% gain in both ImageNet and ImageNet-R. The V-MoE-Base model trained using m2mKD also achieves 3.5% higher accuracy than end-to-end training on ImageNet. The experimental results demonstrate that our method offers a promising solution for connecting modular networks with pretrained monolithic models. Code is available at <https://github.com/kamanphoebe/m2mKD>.

1 Introduction

Despite the remarkable success of large monolithic models in various domains, such as computer vision and natural language processing, concerns have arisen regarding their limited generalization ability and increasing computational costs. In the meantime, there has been a growing interest in modular models, which promise to mitigate the drawbacks of monolithic models. In contrast to monolithic models with fixed computational graphs and parameters, modular neural architectures adapt their parameters to the input, offering favorable properties that are absent in static monolithic models (Han et al., 2022). Unlike monolithic models that collectively optimize parameters, modular models consist of independent modules, and each module can be updated locally without affecting other network parts. These modules are trained to specialize in specific tasks. During inference, only the relevant modules are activated based on the input, even for out-of-distribution samples, thereby enhancing generalization performance (Pfeiffer et al., 2023). For instance, DEMix Layers

^{*} Equal contribution.

[†] Corresponding authors.

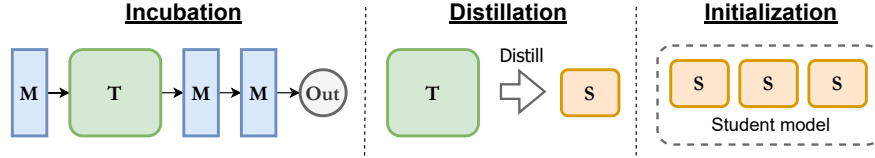


Figure 1: **Overview of m2mKD.** First, incubate the teacher modules T using a meta model M . Then, distill the knowledge from the teacher modules to the student modules. Finally, initialize the modular model with the parameters from the student modules S .

(Gururangan et al., 2022) jointly represent COVID-19-related data using medical and news modules learned from training data. Besides, the conditional calculation in modular models improves computational efficiency. A typical modular architecture, Mixture-of-Experts (MoE) (Shazeer et al., 2017), dramatically scales up model capacity while maintaining similar computational requirements as the original model (Jia et al., 2021; Lepikhin et al., 2021).

Although modular architectures surpass monolithic models in terms of out-of-distribution (OOD) robustness and computational efficiency, there is still vast room for improvement in their algorithms and implementations. Training modular models presents challenges due to optimization difficulties arising from sparse interactions. While recent works (Zoph et al., 2022; Mustafa et al., 2022; Nie et al., 2022) have investigated the training instability of modular models, thorough studies in this area still need to be completed. On the engineering side, several implementations of MoE exist, but many of them (He et al., 2022; Lepikhin et al., 2021) do not consider dynamic workload allocation for experts or support acceleration techniques like mixed precision training. Although adaptive parallelism (Hwang et al., 2023) has addressed the dynamic nature of MoEs, training MoEs remains considerably slower than their monolithic counterparts due to unavoidable communication overheads.

To alleviate the optimization issue, employing a pretrained monolithic model to guide the training of modular models shows potential. **Knowledge distillation (KD)** (Hinton et al., 2015) is an existing technique that transfers knowledge from a pretrained teacher model to a smaller student model. KD has proven effective in the context of monolithic models. However, directly applying conventional KD approaches to modular models is computationally expensive due to their large model sizes. Using a monolithic model as the teacher for a larger modular model may even harm performance (see Table 6). Furthermore, monolithic models trained by regular methods may not be the optimal choice for teachers.

Inspired by the divide-and-conquer training mechanism of Deep Incubation (Ni et al., 2023), we introduce **module-to-module knowledge distillation (m2mKD)** to transfer knowledge between sub-modules of the monolithic teacher and the modular student. As illustrated in Figure 1, we first adopt Deep Incubation, a modular training method, to incubate the teacher modules using a small meta-model. Next, we encourage the student module to imitate the behaviour of the teacher module. Finally, the distilled student modules are used to initialize the modular student model. By adapting the distillation process at the distributed module level, m2mKD significantly reduces the capacity requirement of the teacher model and enables independent training, making distillation less computationally expensive. The cost savings become more noticeable when the modular student is large or when multiple teachers are involved, such as in ensemble learning. Moreover, the teacher model is trained in a modular way, which may benefit teaching a modular student. Note that our m2mKD algorithm does not impose any restrictions on the architecture of both the teacher and student models. We evaluate the performance of m2mKD on both NACs and V-MoE. Experiments show that a NAC model trained using m2mKD improves IID accuracy by approximately 5% on Tiny-ImageNet and enhances out-of-distribution (OOD) robustness by about 4% on Tiny-ImageNet-R. Additionally, there is an average gain of approximately 1% on ImageNet (Deng et al., 2009) and ImageNet-R (Hendrycks et al., 2021a). The experimental results for V-MoE models indicate that m2mKD also works in the case of a small teacher.

Our contributions are as follows: (1) To the best of our knowledge, we are the first to investigate knowledge distillation for modular models. (2) We demonstrate the challenges associated with distilling modular models and introduce a tailored algorithm to address these challenges. (3) Our approach can be seen as a promising framework for transforming a monolithic model into a modular model with arbitrary neural architecture. Notably, this transformation is developed in a modular-style manner. (4) The proposed method is capable of handling irregular distillation scenarios. It has the potential to work not only for the monolithic-to-modular case but also for the monolithic-to-monolithic case. (5) We verify the feasibility of using Deep Incubation for modular models.

2 Related Work

Knowledge Distillation. Knowledge distillation is a model compression technique that transfers knowledge from a large teacher network to a smaller student model (Hinton et al., 2015). Common knowledge distillation approaches involve mimicking the teacher model’s softened output (Hinton et al., 2015; Kim et al., 2018; Ba and Caruana, 2014). In scenarios with multiple teachers, the outputs of all teacher models can be averaged (Hinton et al., 2015), or other methods can be used (Fukuda et al., 2017; Kwon et al., 2020; Yuan et al., 2021). Traditional knowledge distillation methods often struggle when a significant capacity gap exists between the student and the teacher models. Recent approaches have attempted to address this gap by using teacher assistants (Mirzadeh et al., 2019; Son et al., 2021). In addition, some existing works conduct distillation at the module level instead of distilling entire models Xu et al. (2020); Zhao et al. (2022); Liang et al. (2023). While previous works primarily focus on compressing model sizes within the context of monolithic models, we propose a module-to-module distillation technique to enhance the performance of modular architectures, especially in unconventional distillation scenarios. Particularly, the distillation of modules is mutually independent and can be executed in a distributed manner.

Modularization. Modular deep learning involves decomposing neural architectures into independent and parameter-efficient modules, where samples are conditionally routed to subsets of modules, and their outputs are aggregated. Modularization has been widely applied in various areas such as transfer learning (Li and Liang, 2021; Houlsby et al., 2019; Platanios et al., 2018; Hu et al., 2021), modular training (Ni et al., 2023), and scaling up model size (Jia et al., 2021; Lepikhin et al., 2021).

In transfer learning, a common approach is to use pre-trained models as modules in an assembled model for new tasks. The assembled model adapts to new data by adjusting some modules or adding new modules to improve performance in new scenarios. For example, Brown et al. (Brown et al., 2020) added a prompt module to the input of a pre-trained model, and Rebuffi et al. (Rebuffi et al., 2018) introduced adapter modules into the model architecture. In modular training, Deep Incubation (Ni et al., 2023) incubates modules in individual nodes, which avoids communication overhead between nodes and accelerates convergence. Conditional computation allows for scaling up model size while maintaining inference complexity. V-MoE (Jia et al., 2021) scales up vision models with only half the computation required during inference. The MoE framework introduces experts to achieve modularization specifically at the FFN layer. Other modular model architectures include NACs (Weiss et al., 2022) and (Shen et al., 2023; Goyal et al., 2021).

Monolithic to Modular. There are several efforts to convert monolithic models into modular architectures. MoEfication (Zhang et al., acl) directly splits the FFN layers of a monolithic model into multiple experts to form MoE layers, while Sparse Upcycling (Komatsuzaki et al., 2022) copies the MLP parameters to the corresponding experts in the MoE layers. In contrast to these works, our proposed m2mKD does not make assumptions about the model architecture and can be applied to any model.

3 Method

In this section, we first review the essential aspects of Deep Incubation, as our work heavily relies on it. Subsequently, we introduce our proposed method. For convenience, we provide a table (Table 8) that lists the notations commonly used in this paper.

3.1 Preliminary: Deep Incubation

Deep Incubation (Ni et al., 2023) employs a divide-and-conquer strategy to train large models modularly, as illustrated in Figure 2. The process consists of three stages: meta-model pre-training, module incubation, and assembly. In the initial stage, a small model is pre-trained as a meta model using an end-to-end training approach. Subsequently, each module replaces the corresponding layer in the meta-model, and only the module parameters are updated during the incubation process. The incubation of modules is mutually independent and can be completed in a distributed manner. Finally, the incubated modules are assembled and fine-tuned to obtain the final model. It is worth noting that the number of layers in the meta model corresponds to the number of modules incubated during the incubation stage.

3.2 Pipeline

Our method follows a pipeline consisting of three steps (Figure 3): preparation, module-to-module knowledge distillation (m2mKD), and end-to-end (E2E) training. More details are presented below.

Preparation. Prior to commencing the distillation process, the Incubation algorithm is applied to prepare a meta model and a teacher model. This step is actually exclusive of the proposed method. Assuming that the target student model S comprises a total of L modules, the meta model \mathcal{M} should have an equivalent

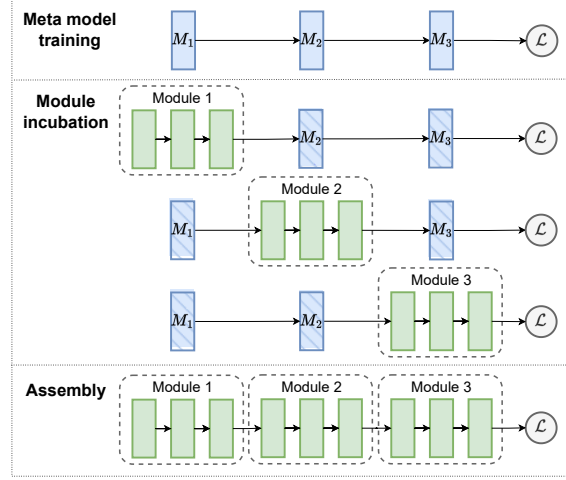


Figure 2: **Overview of Deep Incubation.** Initially, a small model is pre-trained as a meta model. Subsequently, the module replaces the corresponding layer in the meta-model, and only the parameters of the module are updated during incubation. Finally, the incubated modules are assembled and fine-tuned to obtain the final model.

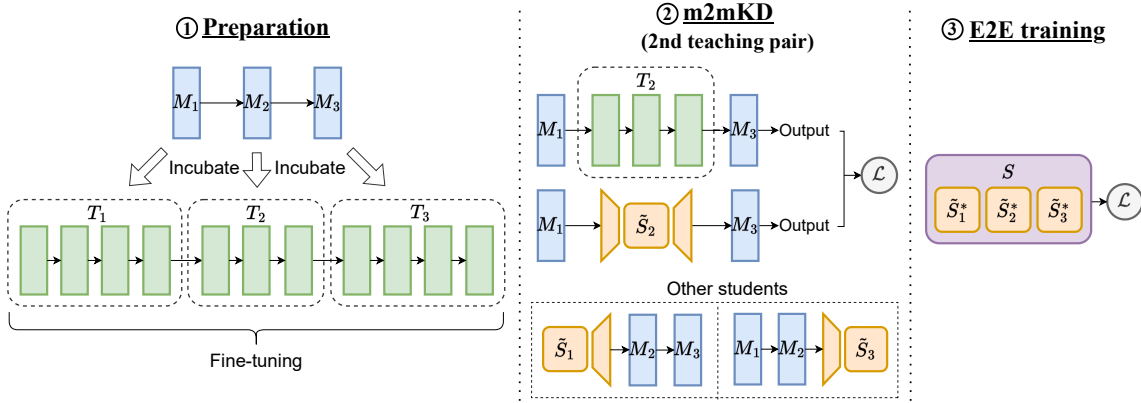


Figure 3: **Pipeline of m2mKD** ($L = 3$). The m2mKD pipeline involves several steps. In the preparation phase, we begin by training a meta model \mathcal{M} , incubating the teacher modules $\{T_i\}$, and fine-tuning the assembled teacher model \mathcal{T} . Subsequently, the m2mKD process is executed as follows: two hybrid networks are constructed by replacing the i -th meta layer M_i with the i -th teaching pair (T_i, \tilde{S}_i) , and their outputs are compared. Note that except for the stitched student module \tilde{S}_i , all other layers are frozen during this phase. Finally, the distilled student modules $\{S_i^*\}$, with stitched layers discarded, are loaded into the student model S at the beginning of the end-to-end training phase.

number of meta layers. Similarly, the teacher model \mathcal{T} , which consists of n layers ($n \geq L$), is divided into L sub-modules:

$$\begin{aligned} S &= S_L \circ S_{L-1} \circ \dots \circ S_1 \\ \mathcal{M} &= M_L \circ M_{L-1} \circ \dots \circ M_1 \\ \mathcal{T} &= T_L \circ T_{L-1} \circ \dots \circ T_1. \end{aligned} \quad (1)$$

As proposed by (Ni et al., 2023), the initial step involves training the meta model in an end-to-end fashion to incubate the L sub-modules T_1, T_2, \dots, T_L . Subsequently, these resulting sub-modules are reassembled to form the teacher model \mathcal{T} , which undergoes fine-tuning. While we follow the same pipeline described in the original paper, our focus is on the sub-modules themselves rather than the entire model. We opt for the Incubation approach instead of merely separating a pre-trained model because we claim that the module incubation phase imparts additional knowledge to the sub-modules. This allows them to learn how to function as individual modules rather than being incomplete fragments of a whole model.

Module-to-module Knowledge Distillation. Once the fine-tuning of the assembled model \mathcal{T} is complete, the sub-modules, or we call “teacher modules” hereafter, are ready for running m2mKD. Unlike traditional knowledge distillation approaches, m2mKD aims to transfer knowledge between modules rather than entire models. Similar to the module incubation proposed by (Ni et al., 2023), we separately link the teacher and student module to the meta model. By comparing the outputs of the two resulting hybrid models, the student modules are encouraged to mimic the behaviour of the corresponding teacher modules. Previous research by Yang et al. (Yang et al., 2022) demonstrates that blocks located at similar depths in different networks can be considered functionally equivalent. This insight suggests that neural networks learn similar patterns at similar network stages. Exploiting this insight, we assign teacher modules to students at the same depth, resulting in L teaching pairs $(T_i, \tilde{S}_i)|i = 1, \dots, L$. Each teaching pair can then be performed m2mKD in parallel. For the i -th teaching pair, we replace the i -th meta layer with T_i and the stitched student module \tilde{S}_i , giving rise to two hybrid networks:

$$\begin{aligned}\tilde{\mathcal{M}}_T^{(i)} &= M_L \circ \dots \circ M_{i+1} \circ T_i \circ M_{i-1} \circ \dots \circ M_1 \\ \tilde{\mathcal{M}}_{\tilde{S}}^{(i)} &= M_L \circ \dots \circ M_{i+1} \circ \tilde{S}_i \circ M_{i-1} \circ \dots \circ M_1.\end{aligned}\quad (2)$$

The modified student module, denoted as \tilde{S}_i , incorporates a linear stitch layer that is inserted right before and/or after the module. This stitch layer is responsible for adjusting the dimension of the feature vectors to address any potential dimension mismatch between the meta layer and the student module. The weight matrix of the pre-stitch layer is denoted as $W \in \mathbb{R}^{d_M \times d_S}$, while the post-stitch layer has a weight matrix denoted as $W \in \mathbb{R}^{d_S \times d_M}$. Here, d_M represents the dimension of the meta layer, and d_S represents the dimension of the student module.

The two hybrid networks are now considered as “complete” models. Consequently, we can directly apply the conventional response-based knowledge distillation technique. Specifically, for the classification problems considered in this paper, we compare the output logits z_T and $z_{\tilde{S}}$ given an input x by measuring the Kullback-Leibler (KL) divergence (Hinton et al., 2015). The total loss \mathcal{L} is then defined as the weighted sum of the classification cross-entropy loss L_{CE} and the knowledge distillation loss L_{KD} :

$$\begin{aligned}\mathcal{L} &= L_{CE} + \alpha L_{KD} \\ L_{CE} &= H(\text{softmax}(z_{\tilde{S}}), y) \\ L_{KD} &= \tau^2 KL(\text{softmax}(z_{\tilde{S}}/\tau), \text{softmax}(z_T/\tau))\end{aligned}\quad (3)$$

where α represents the balancing factor, τ denotes the softmax temperature, and y stands for the label associated with the input x . Throughout the distillation process, only the student module is updated, while both the meta layers and the teacher module remain frozen.

End-to-end training. Given a student model \mathcal{S} consisting of L modules, we can run m2mKD for all teaching pairs $(T_i, \tilde{S}_i)|i = 1, \dots, L$ in parallel to obtain L distilled student modules \tilde{S}_i^* . The last step is to simply load the learned parameters into \mathcal{S} and perform end-to-end (E2E) training. Note that all stitch layers of the student modules are discarded at this stage. For the NAC model architecture, there can be a dimension mismatch problem when loading the learned parameters for certain components, especially if the datasets used in m2mKD and E2E training differ (refer to Section 4.2). In such cases, these incompatible elements will not be loaded.

4 Experiments on NACs

NAC is a novel modular architecture as depicted in Figure 4a. It comprises a read-in layer, multiple propagator layers, and a read-out layer. Modules within two consecutive layers are connected sparsely using Stochastic Kernel Modulated Dot-Product Attention (SKMDPA). The basic computing unit within each module is the ModFC layer, which forms ModFFNs. The majority of parameters are shared across modules, and each module conditions its computation using its own code vector c_u . The SKMDPA mechanism employs sparse attention to calculate the similarity between modules based on their signature vector s_u , thereby determining the communication between modules. Each module maintains a state vector θ_u , which serves as the input for the subsequent layer. The state vector is initialized in the read-in layer, updated through multiple propagator layers, and eventually used as the input for the read-out layer.

4.1 Setups

Datasets. In this paper, we focus on the image classification task. The training for both the preparation and m2mKD phases is conducted using the ImageNet-1k dataset (Deng et al., 2009). For the NAC models,

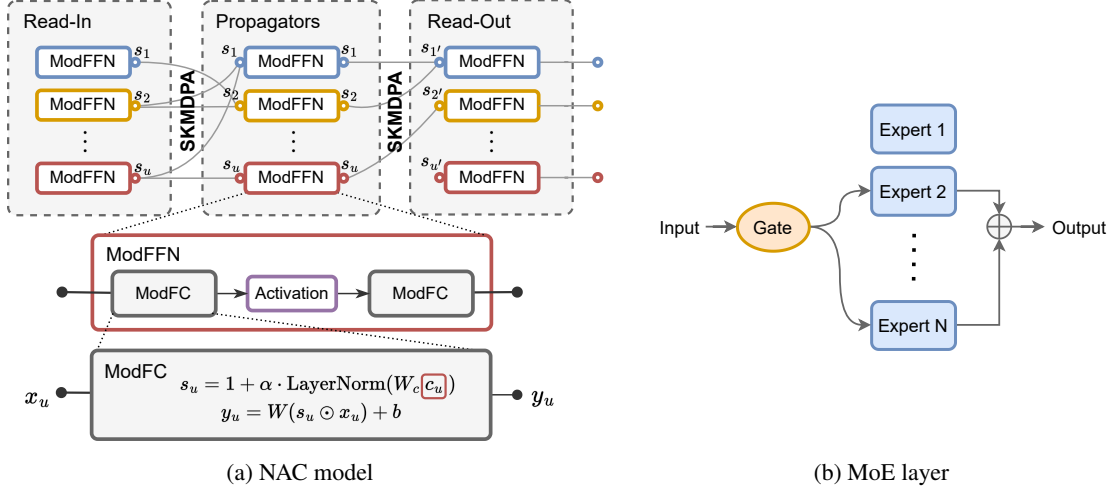


Figure 4: **Overview of the two model architectures used in the experiments.** (a) NAC consists of a read-in layer, multiple propagator layers, and a read-out layer. Each layer of modules is sparsely connected through SKMDPA. The ModFC layer serves as the fundamental computing unit within each module and forms ModFFNs. (b) The MoE layer is constructed using multiple experts and a gate, which selects a specified number of experts (in this case, 2) to process the inputs. The outputs of the selected experts are subsequently aggregated.

we perform end-to-end training using both the ImageNet dataset and its miniature version, Tiny-ImageNet. For OOD evaluation, we utilize the ImageNet-R(enditions) dataset (Hendrycks et al., 2021b) and its down-sampled subset, Tiny-ImageNet-R. Additionally, the CIFAR-100 dataset (Krizhevsky, 2009) is employed for few-shot adaptation.

Preparation. Since our target NAC model consists of a total of 10 layers ($L = 10$), we choose the DeiT-Huge model (Dosovitskiy et al., 2021) with 32 layers as the teacher model to ensure sufficient depth. The DeiT-Huge model is divided into 10 sub-modules, with the first and last sub-modules containing 4 layers each, and the remaining sub-modules comprising 3 layers each. The NAC models contain no more than 37M parameters, while the DeiT-Huge model contains 632M parameters. This yields approximately 3.7M and 63.2M parameters for each student and teacher module, respectively. At the beginning of the preparation stage, a 10-layer meta model is trained on ImageNet for 300 epochs. Subsequently, each teacher module is incubated by the meta model for 100 epochs, and all modules are assembled back together for additional fine-tuning of 100 epochs. The training configurations for this stage are identical to the Deep Incubation approach.

m2mKD. When the teacher part is hidden, m2mKD can be seen as module incubation with an additional loss term. Therefore, we again adopt similar experimental settings from module incubation for m2mKD. The only difference is that each student module is trained for just 10 epochs. We set the balancing factor α to 0.5 and the softmax temperature τ to 1.0. Given the dimension of the meta model $d_M = 1280$ and of the student modules $d_S = 384$ for Tiny-ImageNet¹ (or $d_S = 512$ for ImageNet), there would be 1M parameters for each pair of stitch layers. After connecting the student and teacher modules with meta layers, the resulting hybrid networks $\tilde{M}_S^{(i)}$ and $\tilde{M}_T^{(i)}$ contain 182.5M and 242.0M parameters, respectively.

Originally, the NAC propagator layers receive the state vectors of the previous layer as inputs and update the states after the computation of SKMDPA and ModFFN. However, we remove the SKMDPA part for our student modules, allowing all modules to communicate with each other. This modification is made for two reasons: (1) The signature vectors which determine the communication probability between modules are shared across depths. Even though we learn a set of signature vectors for each student module, they cannot be reused during the end-to-end training of NAC models. (2) The inputs of the student modules are changed to be the feature vectors from the meta layers and no longer represent the states of modules. These inputs contain all the necessary information, and none of them should be omitted. To ensure that the ModFC layers function properly, we randomly initialize the state and code vectors. Note that these vectors are neither updated during

¹The dataset here refers to the one used in the E2E training phase.

Table 1: **IID and OOD performance of NACs trained on Tiny-ImageNet.** Our m2mKD approach is compared against the original end-to-end training.

		IID (Tiny-ImageNet Validation)		OOD (Tiny-ImageNet-R)	
		Acc@1	Acc@5	Acc@1	Acc@5
NACs	with Scale-Free Prior	60.83	82.35	20.74	41.71
	with Planted-Partition Prior	60.57	82.20	20.50	42.94
	with Ring-of-Cliques Prior	60.70	82.57	20.89	41.80
	with Erdos-Renyi Prior	61.53	83.14	21.08	42.25
+m2mKD	with Scale-Free Prior	66.47 (+5.64)	85.08 (+2.73)	24.31 (+3.57)	44.38 (+2.67)
	with Planted-Partition Prior	66.04 (+5.47)	85.68 (+3.48)	24.69 (+4.19)	45.36 (+2.42)
	with Ring-of-Cliques Prior	66.21 (+5.51)	85.49 (+2.92)	24.89 (+4.00)	45.74 (+3.94)
	with Erdos-Renyi Prior	65.99 (+4.46)	85.37 (+2.23)	24.54 (+3.46)	45.45 (+3.20)

the distillation process nor loaded into the target model for the end-to-end training. Specifically, \tilde{S}_1 consists of the input tokenizer and the read-in layer, $\tilde{S}_{i=2,\dots,L-1}$ consists of the i -th modified propagator layer, and \tilde{S}_L includes both the modified read-out layer and the output tokenizer.

E2E training. When training on the same dataset, the hyperparameters remain unchanged for both the reproduced baselines and the distilled NAC models. However, since the original paper on NACs does not provide a comprehensive list of hyperparameters and we were unable to reproduce the reported results using the given hyperparameters, we adjusted some of them in order to approach their reported results as closely as possible. Table 9 presents a selection of our hyperparameters², including all altered values.

4.2 Results

Main results. As aforementioned, our teacher model DeiT-Huge and NAC student modules in the first two phases are trained solely on ImageNet. The assembled teacher model achieves a validation accuracy of 81.8%. With 8 A100 80GB GPUs, the training of m2mKD for all ten student modules can be completed within 12 hours. For E2E training on Tiny-ImageNet, a portion of the input tokenizer and the entire output tokenizer in the student modules need to be discarded due to dimension mismatching. Table 1 compares the reproduced baselines and our distilled NAC models on Tiny-ImageNet and Tiny-ImageNet-R. The reproduced results slightly outperform the reported values in the original paper. Although the dataset is different from the one used in the m2mKD phase, our distilled models with various graph prior regularizers exhibit an average improvement of 5.3% in IID performance and 3.8% in OOD robustness over the baselines. This indicates that the addition of distilled student modules not only enhances the ability of the final NAC for similar tasks, but also improves its modularity. To ensure reproducibility, we repeat the E2E training phase of the distilled model with scale-free prior three times and measure their mean and standard deviation. The results are presented in Table 2.

The comparison for ImageNet is shown in Table 3. The original paper only provides the validation accuracy of the NAC trained on ImageNet with a scale-free graph prior, which is 77%. We reproduce the baselines for all four graph priors, with the maximum value being 76.1%. Our distilled NACs achieve maximum gains of 1.0% and 2.4% for IID and OOD performance, respectively.

Few-shot. To evaluate the few-shot adaptation performance, we further fine-tune the classifier layer of the distilled NAC with a scale-free prior, which is trained on ImageNet, using a small number of samples from the CIFAR-100 dataset. The hyperparameters are listed in Table 10, and the results are presented in Table 4. We conduct the experiments with 5 different seeds and report the averaged accuracies and corresponding standard deviations in Figure 5. Our reproduced baselines are at most 10% higher than the original results. It can be observed that the distilled model performs similarly to the baseline with no significant improvement. The standard deviations are relatively large, possibly due to the limited number of repetitions (i.e., the number of seeds). We also rerun the 2-shot experiments once for all five seeds to examine the variation under the same seeds. Table 5 shows that given a fixed seed, the largest difference is around 7%. Therefore, additional experiments may be necessary to further validate the few-shot performance.

²For the full list of hyperparameters, please refer to the configuration files provided on GitHub.

Table 2: **Mean and standard deviation of experimental results of NACs trained by m2mKD on Tiny-ImageNet.** We repeat the end-to-end training phase of a distilled NAC model with a scale-free prior three times and calculate the mean and standard deviation of IID and OOD performance.

	IID		OOD	
	Acc@1	Acc@5	Acc@1	Acc@5
1st	66.47	85.08	24.31	44.38
2nd	66.13	85.33	24.84	45.00
3rd	65.94	85.49	25.29	45.61
MEAN	66.18	85.30	24.81	45.00
STDEV	0.27	0.21	0.49	0.62

Table 3: **IID and OOD performance of NACs trained on ImageNet.** Our m2mKD approach is compared against the original end-to-end training.

		IID (ImageNet Validation)		OOD (ImageNet-R)	
		Acc@1	Acc@5	Acc@1	Acc@5
NACs	with Scale-Free Prior	75.61	93.93	37.30	54.01
	with Planted-Partition Prior	75.71	94.09	37.63	54.38
	with Ring-of-Cliques Prior	76.12	94.35	37.21	53.70
	with Erdos-Renyi Prior	75.71	93.95	36.48	53.39
+m2mKD	with Scale-Free Prior	76.63 (+1.02)	94.62 (+0.69)	39.18 (+1.88)	55.10 (1.09)
	with Planted-Partition Prior	76.49 (+0.78)	94.01 (-0.08)	38.02 (+0.39)	53.58 (-0.8)
	with Ring-of-Cliques Prior	76.89 (+0.77)	94.44 (+0.09)	39.29 (+2.08)	55.42 (+1.72)
	with Erdos-Renyi Prior	76.56 (+0.85)	94.39 (+0.44)	38.84 (+2.36)	54.69 (+1.3)

5 Experiments on MoEs

In a MoE model, some or all of the feedforward networks (FFNs) in a standard monolithic model are replaced with MoE layers. As illustrated in Figure 4b, a MoE layer is constructed by multiple experts and a gate, where each expert is essentially an FFN. The gate, typically implemented as a MLP, is responsible for selecting a specified number of experts to process the input. The outputs of the selected experts are then aggregated. The computation performed by a MoE layer can be expressed as (Shazeer et al., 2017):

$$y = \sum_{i=1}^n G(x)_i E_i(x)$$

where n denotes the total number of experts, $E_i(\cdot)$ represents the output of the i -th expert, and $G(\cdot)_i$ denotes the score computed by the gate for the i -th expert.

5.1 Setups

Datasets. We exclusively used the ImageNet-1k dataset for MoE models throughout the pipeline (from preparation to E2E training). The few-shot adaptation ability is evaluated on both CIFAR-100 and CUB-2011 datasets (Wah et al., 2011).

Preparation. We choose a DeiT-Large model with 24 layers and 304M parameters as the teacher model. Instead of training the meta model and the teacher model from scratch, we utilize the released checkpoints of Deep Incubation, which achieve an accuracy of 83.9% on ImageNet-1k. The teacher model is evenly divided into $L = 4$ sub-modules, each consisting of 6 layers. The meta model is a four-layer DeiT model with the same embedded dimension as the teacher model.

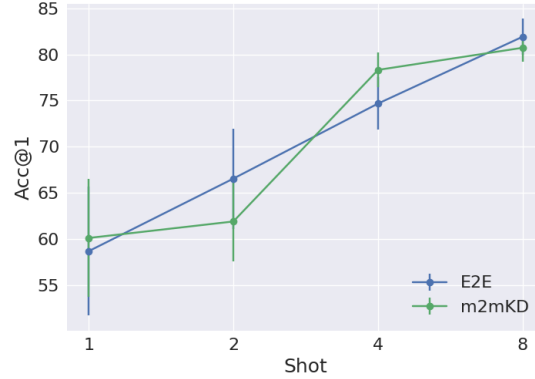
m2mKD. In this series of experiments, the target model S is set as a Vision MoE Base (V-MoE-B) model (Riquelme et al., 2021). Instead of using the carefully designed gate proposed by (Riquelme et al., 2021), we employ the earliest introduced gate in (Shazeer et al., 2017) which purely performs a top- k ($k = 2$) operation and no additional constraint or balancing loss is applied:

$$Gate(x) = Softmax(TopK(W \cdot x)).$$

Our V-MoE-B model is composed of 12 MoE layers (i.e., all feed-forward layers in a DeiT-B are changed to MoE layers) and each of them contains 8 experts. Hence, there are a total of 483M parameters in the

Table 4: **Few-shot performance of NACs on CIFAR-100.** The model is tasked with classifying the samples into 8 classes (i.e. 8-way).

Seed	1-shot		2-shot		4-shot		8-shot	
	E2E	m2mKD	E2E	m2mKD	E2E	m2mKD	E2E	m2mKD
1	53.66	60.82	64.39	64.39	71.21	75.06	81.03	80.53
2	60.82	50.08	64.39	59.03	75.06	78.91	84.04	82.03
3	67.97	67.97	75.13	67.97	78.91	79.87	80.53	79.03
4	60.82	60.82	67.97	57.24	75.06	78.91	84.04	82.53
5	50.08	60.82	60.82	60.82	73.14	78.91	80.03	79.53
MEAN	58.67	60.10	66.54	61.89	74.68	78.33	81.93	80.73
STDEV	6.98	6.40	5.43	4.31	2.85	1.88	1.95	1.52

Figure 5: **Few-shot performance of NACs on CIFAR-100.**Table 5: **Differences between two runs of the 2-shot experiment on NACs.**

seed	E2E			m2mKD		
	1st	2nd	$ \Delta $	1st	2nd	$ \Delta $
1	64.39	69.76	5.37	64.39	66.18	1.79
2	64.39	64.39	0.00	59.03	60.82	1.79
3	75.13	75.13	0.00	67.97	75.13	7.16
4	67.97	66.18	1.79	57.24	62.60	5.36
5	60.82	62.60	1.78	60.82	64.39	3.57
MEAN	66.54	67.61	1.07	61.89	65.82	3.93
STDEV	5.43	4.97	0.46	4.31	5.57	1.26

student model. Note that the student model size is larger than the teacher model size. Each three layers of the V-MoE-B model are grouped as a student module, resulting in a total of 4 student modules. In this case, we have $d_M = 1024$ and $d_S = 768$, and thus a pair of stitch layers accounts for about 1.6M parameters. As a result, there are around 122.4M parameters for each student module and 77.6M parameters for each teacher module. The two hybrid networks $\tilde{M}_S^{(i)}$ and $\tilde{M}_T^{(i)}$ constructed in this phase will then comprise 160.5M and 115.9M parameters respectively.

Unlike the NAC models, the student modules of MoE do not require modification, and all of their learned parameters can be loaded into the target model during the end-to-end training phase. The same as the settings for NAC models, we set the balancing factor $\alpha = 0.5$ and softmax temperature $\tau = 1.0$. All of the remaining hyperparameters are identical to those used in Deep Incubation for incubating DeiT-B (Touvron et al., 2021) and the student modules are trained for 100 epochs.

E2E training. Again, we adopt the same set of hyperparameters as Deep Incubation to train the V-MoE-B model, except for the update frequency argument, which is set to half of the original value.

5.2 Results

Main results. We compare m2mKD with three baselines: pure end-to-end training, conventional knowledge distillation, and Deep Incubation. For end-to-end training, we train a V-MoE-B model from scratch for 300 epochs using the same hyperparameters as in the DeiT-B training (Touvron et al., 2021). In contrast to m2mKD, which performs knowledge distillation at the module level, conventional KD refers to knowledge distillation between complete models. For the sake of fair comparison, we again use DeiT-L as the teacher model and V-MoE-B as the student model. The KL divergence between their output logits is incorporated into the loss with $\alpha = 0.5$ and $\tau = 1.0$ (see Equation 3). The training process lasts for 300 epochs. Lastly, we consider the original Deep Incubation approach, where we use their open source checkpoint of the meta model, originally trained for incubating DeiT-B, for the V-MoE-B experiments. The validation results on ImageNet-1k are summarized in Table 6. Conventional KD underperforms the other methods, with an accuracy 1.9% lower than pure end-to-end training, which is the second lowest. This verifies our assertion that existing knowledge distillation techniques are not necessarily compatible with modular models. On the other hand, the Deep Incubation approach achieves 2.97% higher accuracy than end-to-end training, demonstrating its effectiveness not only for monolithic models, but also for modular models. Our m2mKD approach further increases the accuracy by 0.50%, resulting in the best performance among these methods. Given the remarkable OOD results of NACs in previous experiments, we also investigate the OOD robustness of MoEs on the ImageNet-R dataset, which is rare to be discussed in other MoE-related literatures. Surprisingly, all the MoE models trained using the four different methods achieve near 0% accuracy on the ImageNet-R dataset. Based on these experiments, it appears that NACs are significantly stronger than MoEs in terms of OOD or zero-shot performance.

Training time. In addition to accuracy, Table 6 presents the ratios of training time calculated relative to the time taken by the pure end-to-end training approach. m2mKD is slightly slower than Deep Incubation but roughly equivalent to the pure end-to-end method in terms of time, while conventional KD requires $1.12\times$ time. Further experiments (Appendix C) demonstrate that the ratio for m2mKD can be reduced to 0.57 with marginal performance degradation. For a fair comparison, we exclude the duration of teacher model training for the KD and m2mKD methods. In other words, only the time for meta model training, distillation, and end-to-end training phases are considered in the time calculation for m2mKD. At this point, it is natural to question whether the preparation phase of m2mKD can be simplified. The current m2mKD pipeline involves incubating a teacher model in the preparation phase. We suppose that such a model would be a more knowledgeable teacher specifically for modular students. However, since numerous pretrained models are publicly available, it would be time-saving to utilize them as the teacher model for m2mKD instead of training a new one from scratch. If this approach is adopted, the total training time would be exactly as stated in the table. We leave the investigation of how teachers trained using different methods influence the performance of m2mKD in future work.

Few-shot. We evaluate the few-shot adaptation of three models: a DeiT-B model trained using Deep Incubation, and two V-MoE-B models trained using Deep Incubation and m2mKD, respectively. The hyperparameters can be found in Table 10. During the few-shot training, all parameters in these models are frozen, except for the newly random initialized classifier layer, whose output dimension is set to the number of few-shot classes (8 in all experiments). The experiments for each shot are repeated with five different seeds. In Table 7, we report the highest accuracy achieved within 100 epochs for each experiment, along with the mean and standard deviation calculated over the seeds. The averaged results are also depicted in Figure 6. Surprisingly, the DeiT-B model outperforms both V-MoE-B models, which are expected to be capable due to their modularity. This might be attributed to the relatively small dataset size (ImageNet-1k), resulting in insufficient training samples for each expert to learn comprehensively. However, when focusing on the two MoE models, the one trained using m2mKD consistently outperforms the Incubation model by approximately 2% for all shots on

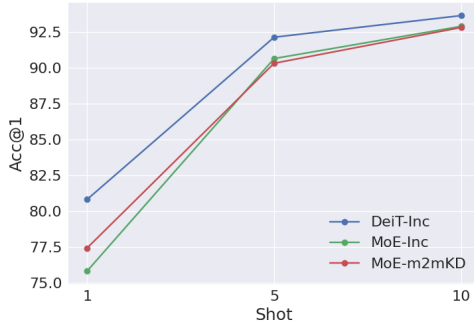
Table 6: **Performance of V-MoE-B models trained using different approaches on ImageNet-1k.** Baselines include pure end-to-end training (pure E2E), conventional knowledge distillation (KD), and Deep Incubation.

	Acc@1	Acc@5	Ratio of Time
Pure E2E	78.43	93.47	1.00
KD	76.53	92.65	1.12
Incubation	81.40	95.06	0.91
m2mKD	81.90	95.43	0.99

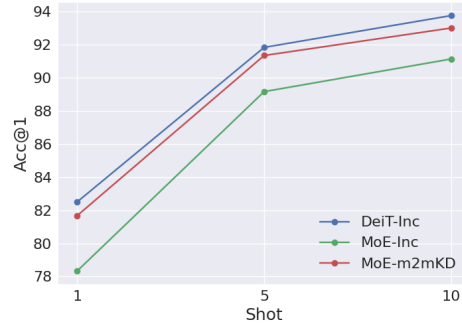
Table 7: **Few-shot performance of DeiT and V-MoE-B models on CIFAR-100 (top) and CUB-2011 (bottom).** The models are tasked with classifying samples into 8 classes (i.e., 8-way). We compare three models: a DeiT-B model trained using Deep Incubation (DeiT-Inc), and two V-MoE-B models trained using Deep Incubation (MoE-Inc) and m2mKD (MoE-m2mKD), respectively.

CIFAR-100									
Seed	1-shot			5-shot			10-shot		
	DeiT-Inc	MoE-Inc	MoE-m2mKD	DeiT-Inc	MoE-Inc	MoE-m2mKD	DeiT-Inc	MoE-Inc	MoE-m2mKD
1	70.83	70.83	70.83	90.83	90.00	89.17	90.83	91.67	90.42
2	70.83	62.50	66.37	90.00	87.50	86.67	92.92	92.50	90.42
3	87.50	95.83	91.67	95.83	94.17	94.17	97.08	96.25	96.67
4	95.83	79.17	87.50	95.83	94.17	94.17	97.50	94.58	96.25
5	79.17	70.83	70.83	88.33	87.50	87.50	90.00	89.58	90.42
MEAN	80.83	75.83	77.44	92.16	90.67	90.34	93.67	92.92	92.84
STDEV	10.87	12.64	11.33	3.47	3.36	3.61	3.48	2.59	3.31

CUB-2011									
Seed	1-shot			5-shot			10-shot		
	DeiT-Inc	MoE-Inc	MoE-m2mKD	DeiT-Inc	MoE-Inc	MoE-m2mKD	DeiT-Inc	MoE-Inc	MoE-m2mKD
1	83.33	70.83	70.83	90.83	90.83	91.67	95.00	94.38	93.75
2	79.17	83.33	87.5	94.17	93.33	94.17	98.75	95.63	98.13
3	95.83	91.67	95.83	95.00	92.50	92.50	94.38	91.25	91.25
4	87.50	75.00	79.17	88.33	80.83	84.17	84.38	80.63	86.25
5	66.67	70.83	75.00	90.83	88.33	94.17	96.25	93.75	95.63
MEAN	82.50	78.33	81.67	91.83	89.16	91.34	93.75	91.13	93.00
STDEV	10.78	9.04	10.03	2.73	5.04	4.15	5.50	6.08	4.54



(a) CIFAR-100 8 way



(b) CUB-2011 8 way

Figure 6: **Few-shot performance of DeiT and V-MoE-B models on CIFAR-100 (left) and CUB-100 (right).**

CUB-2011, as well as the 1-shot experiment on CIFAR-100. Similar to the few-shot results of NACs (Section 4.2), the standard deviations are relatively large. Conducting experiments on a larger dataset is necessary to obtain a more precise evaluation of the few-shot performance.

Ablations. In the proposed m2mKD pipeline, the stitch layers are used only during the distillation phase and subsequently discarded to ensure no modifications are required for the student model. Although the stitch layers typically account for just a small proportion of the total parameters in a large modular model (e.g., 1% for our V-MoE-B student), directly removing them may result in the loss of some knowledge acquired from the teacher, potentially impacting the final model’s performance negatively. To investigate this aspect, we conduct additional experiments by preserving the stitch layers in the student model. These experiments include decreasing the number of distillation epochs for m2mKD and scaling up. For further details, please refer to Appendix C.

6 Conclusion and Future works

In this work, we present module-to-module knowledge distillation (m2mKD) as a general approach for transferring knowledge in the context of modular model training. m2mKD leverages a monolithic teacher model to

facilitate the training of a modular student model, offering a promising strategy for transforming pretrained monolithic models into modular architectures to harness their advantages. Experimental results on NACs and MoEs demonstrate that the proposed pipeline effectively enhances the IID accuracy and OOD robustness of modular models, even in scenarios where the student model size is smaller than the teacher model size. However, there is still room for improvement in bridging the performance gap between the student modular model and the teacher model. To further enhance the effectiveness, m2mKD can be combined with existing techniques such as ensemble learning. We hope that this work will advance research on module-wise knowledge distillation and monolithic-to-modular conversion, and we look forward to future studies in these areas.

References

- Ba, J. and Caruana, R. (2014). Do deep nets really need to be deep? In Ghahramani, Z., Welling, M., Cortes, C., Lawrence, N., and Weinberger, K., editors, *Advances in Neural Information Processing Systems*, volume 27. Curran Associates, Inc.
- Brown, T. B., Mann, B., Ryder, N., Subbiah, M., Kaplan, J., Dhariwal, P., Neelakantan, A., Shyam, P., Sastry, G., Askell, A., Agarwal, S., Herbert-Voss, A., Krueger, G., Henighan, T., Child, R., Ramesh, A., Ziegler, D. M., Wu, J., Winter, C., Hesse, C., Chen, M., Sigler, E., Litwin, M., Gray, S., Chess, B., Clark, J., Berner, C., McCandlish, S., Radford, A., Sutskever, I., and Amodei, D. (2020). Language models are few-shot learners. *arXiv preprint arXiv: 2005.14165*.
- Deng, J., Dong, W., Socher, R., Li, L.-J., Li, K., and Fei-Fei, L. (2009). Imagenet: A large-scale hierarchical image database. In *2009 IEEE Conference on Computer Vision and Pattern Recognition*, pages 248–255.
- Dosovitskiy, A., Beyer, L., Kolesnikov, A., Weissenborn, D., Zhai, X., Unterthiner, T., Dehghani, M., Minderer, M., Heigold, G., Gelly, S., Uszkoreit, J., and Houlsby, N. (2021). An Image is Worth 16x16 Words: Transformers for Image Recognition at Scale. *arXiv:2010.11929 [cs]*.
- Fukuda, T., Suzuki, M., Kurata, G., Thomas, S., Cui, J., and Ramabhadran, B. (2017). Efficient knowledge distillation from an ensemble of teachers. In *Interspeech*.
- Goyal, A., Didolkar, A., Lamb, A., Badola, K., Ke, N. R., Rahaman, N., Binas, J., Blundell, C., Mozer, M. C., and Bengio, Y. (2021). Coordination among neural modules through a shared global workspace. *ArXiv*, abs/2103.01197.
- Gururangan, S., Lewis, M., Holtzman, A., Smith, N. A., and Zettlemoyer, L. (2022). DEMix layers: Disentangling domains for modular language modeling. In *Proceedings of the 2022 Conference of the North American Chapter of the Association for Computational Linguistics: Human Language Technologies*, pages 5557–5576, Seattle, United States. Association for Computational Linguistics.
- Han, Y., Huang, G., Song, S., Yang, L., Wang, H., and Wang, Y. (2022). Dynamic neural networks: A survey. *IEEE Transactions on Pattern Analysis & Machine Intelligence*, 44(11):7436–7456.
- He, J., Zhai, J., Antunes, T., Wang, H., Luo, F., Shi, S., and Li, Q. (2022). Fastermoe: Modeling and optimizing training of large-scale dynamic pre-trained models. In *Proceedings of the 27th ACM SIGPLAN Symposium on Principles and Practice of Parallel Programming, PPOPP ’22*, page 120–134, New York, NY, USA. Association for Computing Machinery.
- Hendrycks, D., Basart, S., Mu, N., Kadavath, S., Wang, F., Dorundo, E., Desai, R., Zhu, T., Parajuli, S., Guo, M., Song, D., Steinhardt, J., and Gilmer, J. (2021a). The many faces of robustness: A critical analysis of out-of-distribution generalization.
- Hendrycks, D., Basart, S., Mu, N., Kadavath, S., Wang, F., Dorundo, E., Desai, R., Zhu, T., Parajuli, S., Guo, M., Song, D., Steinhardt, J., and Gilmer, J. (2021b). The many faces of robustness: A critical analysis of out-of-distribution generalization. *ICCV*.
- Hinton, G., Vinyals, O., and Dean, J. (2015). Distilling the knowledge in a neural network.
- Houlsby, N., Giurghi, A., Jastrzebski, S., Morrone, B., de Laroussilhe, Q., Gesmundo, A., Attariyan, M., and Gelly, S. (2019). Parameter-efficient transfer learning for nlp. *arXiv preprint arXiv: 1902.00751*.
- Hu, J., Shen, Y., Wallis, P., Allen-Zhu, Z., Li, Y., Wang, S., and Chen, W. (2021). Lora: Low-rank adaptation of large language models. *International Conference On Learning Representations*.
- Hwang, C., Cui, W., Xiong, Y., Yang, Z., Liu, Z., Hu, H., Wang, Z., Salas, R., Jose, J., Ram, P., Chau, J., Cheng, P., Yang, F., Yang, M., and Xiong, Y. (2023). Tutel: Adaptive mixture-of-experts at scale.

- Jia, C., Yang, Y., Xia, Y., Chen, Y., Parekh, Z., Pham, H., Le, Q. V., Sung, Y., Li, Z., and Duerig, T. (2021). Scaling up visual and vision-language representation learning with noisy text supervision. In Meila, M. and Zhang, T., editors, *Proceedings of the 38th International Conference on Machine Learning, ICML 2021, 18-24 July 2021, Virtual Event*, volume 139 of *Proceedings of Machine Learning Research*, pages 4904–4916. PMLR.
- Kim, J., Park, S., and Kwak, N. (2018). Paraphrasing complex network: network compression via factor transfer. In *Proceedings of the 32nd International Conference on Neural Information Processing Systems*, pages 2765–2774.
- Komatsuzaki, A., Puigcerver, J., Lee-Thorp, J., Ruiz, C. R., Mustafa, B., Ainslie, J., Tay, Y., Dehghani, M., and Houlsby, N. (2022). Sparse upcycling: Training mixture-of-experts from dense checkpoints. *International Conference on Learning Representations*.
- Krizhevsky, A. (2009). Learning multiple layers of features from tiny images. pages 32–33.
- Kwon, K., Na, H., Lee, H., and Kim, N. S. (2020). Adaptive knowledge distillation based on entropy. In *ICASSP 2020 - 2020 IEEE International Conference on Acoustics, Speech and Signal Processing (ICASSP)*, pages 7409–7413.
- Lepikhin, D., Lee, H., Xu, Y., Chen, D., Firat, O., Huang, Y., Krikun, M., Shazeer, N., and Chen, Z. (2021). Gshard: Scaling giant models with conditional computation and automatic sharding. In *9th International Conference on Learning Representations, ICLR 2021, Virtual Event, Austria, May 3-7, 2021*. OpenReview.net.
- Li, X. L. and Liang, P. (2021). Prefix-tuning: Optimizing continuous prompts for generation. *Annual Meeting Of The Association For Computational Linguistics*.
- Liang, C., Yu, J., Yang, M.-H., Brown, M., Cui, Y., Zhao, T., Gong, B., and Zhou, T. (2023). Module-wise adaptive distillation for multimodality foundation models.
- Mirzadeh, S.-I., Farajtabar, M., Li, A., and Ghasemzadeh, H. (2019). Improved knowledge distillation via teacher assistant: Bridging the gap between student and teacher. *arXiv preprint arXiv:1902.03393*.
- Mustafa, B., Riquelme, C., Puigcerver, J., Jenatton, R., and Houlsby, N. (2022). Multimodal contrastive learning with limoe: the language-image mixture of experts.
- Ni, Z., Wang, Y., Yu, J., Jiang, H., Cao, Y., and Huang, G. (2023). Deep Incubation: Training Large Models by Divide-and-Conquering. *arXiv:2212.04129 [cs]*.
- Nie, X., Miao, X., Cao, S., Ma, L., Liu, Q., Xue, J., Miao, Y., Liu, Y., Yang, Z., and Cui, B. (2022). Evomoe: An evolutionary mixture-of-experts training framework via dense-to-sparse gate.
- Pfeiffer, J., Ruder, S., Vulić, I., and Ponti, E. M. (2023). Modular deep learning. *arXiv preprint arXiv: Arxiv-2302.11529*.
- Platanios, E. A., Sachan, M., Neubig, G., and Mitchell, T. (2018). Contextual parameter generation for universal neural machine translation. *arXiv preprint arXiv: 1808.08493*.
- Rebuffi, S.-A., Bilen, H., and Vedaldi, A. (2018). Efficient parametrization of multi-domain deep neural networks. *arXiv preprint arXiv: 1803.10082*.
- Riquelme, C., Puigcerver, J., Mustafa, B., Neumann, M., Jenatton, R., Susano Pinto, A., Keysers, D., and Houlsby, N. (2021). Scaling vision with sparse mixture of experts. In Ranzato, M., Beygelzimer, A., Dauphin, Y., Liang, P., and Vaughan, J. W., editors, *Advances in Neural Information Processing Systems*, volume 34, pages 8583–8595. Curran Associates, Inc.
- Shazeer, N., Mirhoseini, A., Maziarz, K., Davis, A., Le, Q., Hinton, G., and Dean, J. (2017). Outrageously large neural networks: The sparsely-gated mixture-of-experts layer.
- Shen, Y., Zhang, Z., Cao, T., Tan, S., Chen, Z., and Gan, C. (2023). Moduleformer: Learning modular large language models from uncurated data. *arXiv preprint arXiv: 2306.04640*.
- Son, W., Na, J., Choi, J., and Hwang, W. (2021). Densely guided knowledge distillation using multiple teacher assistants. In *2021 IEEE/CVF International Conference on Computer Vision (ICCV)*, pages 9375–9384.
- Touvron, H., Cord, M., Douze, M., Massa, F., Sablayrolles, A., and Jegou, H. (2021). Training data-efficient image transformers & distillation through attention. In Meila, M. and Zhang, T., editors, *Proceedings of*

- the 38th International Conference on Machine Learning*, volume 139 of *Proceedings of Machine Learning Research*, pages 10347–10357. PMLR.
- Wah, C., Branson, S., Welinder, P., Perona, P., and Belongie, S. (2011). *The Caltech-UCSD Birds-200-2011 Dataset*.
- Weiss, M., Rahaman, N., Locatello, F., Pal, C., Bengio, Y., Schölkopf, B., Li, L. E., and Ballas, N. (2022). Neural Attentive Circuits.
- Xu, C., Zhou, W., Ge, T., Wei, F., and Zhou, M. (2020). Bert-of-theseus: Compressing bert by progressive module replacing. In *Conference on Empirical Methods in Natural Language Processing*.
- Yang, X., Zhou, D., Liu, S., Ye, J., and Wang, X. (2022). Deep model reassembly. *arXiv preprint arXiv:2210.17409*.
- Yuan, F., Shou, L., Pei, J., Lin, W., Gong, M., Fu, Y., and Jiang, D. (2021). Reinforced multi-teacher selection for knowledge distillation. *Proceedings of the AAAI Conference on Artificial Intelligence*, 35(16):14284–14291.
- Zhang, Z., Lin, Y., Liu, Z., Li, P., Sun, M., and Zhou, J. (acl). Moefication: Transformer feed-forward layers are mixtures of experts. *FINDINGS*.
- Zhao, K., Nguyen, H., Jain, A., Susanj, N., Mouchtaris, A., Gupta, L., and Zhao, M. (2022). Knowledge Distillation via Module Replacing for Automatic Speech Recognition with Recurrent Neural Network Transducer. In *Proc. Interspeech 2022*, pages 4436–4440.
- Zoph, B., Bello, I., Kumar, S., Du, N., Huang, Y., Dean, J., Shazeer, N. M., and Fedus, W. (2022). St-moe: Designing stable and transferable sparse expert models.

A Notations

Table 8: **Notations.**

Symbol	Definition
\mathcal{T}	Teacher model
T_i	The i -th teacher module
\mathcal{M}	Meta model
M_i	The i -th meta layer
\mathcal{S}	Student model
S_i	The i -th student module
\tilde{S}_i	The i -th stitched student module
L	Number of student modules
d_M	Dimension of meta model which decides the size of stitch layers ($d_M \times d_S$)
d_S	Dimension of student model which decides the size of stitch layers ($d_M \times d_S$)
c_u	Code vector of the u -th module in a NACs model
s_u	Signature vector of the u -th module in a NACs model
θ_u	State vector of the u -th module in a NACs model

B Training Hyperparameters

Table 9: **Hyperparameters for the E2E training phase of NACs.**

Hyperparameter	Tiny-ImageNet	ImageNet
Batch size	1024	256
Number of epochs	400	110
Optimizer	AdamW	AdamW
Weight decay	0.075	0.05
Learning rate scheduler	Cosine	Cosine
Warmup epochs	25	25
Warmup from learning rate	1e-6	1e-6
Base peak learning rate	$0.0012 \times \frac{\text{batchsize}}{512}$	$0.0012 \times \frac{\text{batchsize}}{512}$
Base min learning rate	$4e-5 \times \frac{\text{batchsize}}{512}$	$4e-5 \times \frac{\text{batchsize}}{512}$
Dimension of state	384	512
Propagator layers	8	8
Processor modules	320	960
- Input modules	64	192
- Propagator modules	256	768
Attention heads	6	8
Read-in heads	6	8
Activation function	GEGLU	GEGLU
FFN hidden units	1536	1024
Output modules	64	64
Signature dimension	64	64
Code dimension	384	512
Sampling temperature	0.5	0.5
Kernel bandwidth	1.0	1.0
Modulation at initialization	0.1	0.1

Table 10: **Hyperparameters for the few-shot training of NACs, DeiT and V-MoE-B models.**

	NACs	DeiT / V-MoE-B
Batch size	$8 \times \text{shot}$	$8 \times \text{shot}$
Number of epochs	500	100
Optimizer	SGD	AdamW
Weight decay	0.0	0.05
Learning rate scheduler	None	Cosine
(Peak) Learning rate	0.0003	0.002
Min learning rate	N/A	$1e-5$
Momentum	0.9	N/A
Warmup epochs	N/A	20
Warmup from learning rate	N/A	$1e-6$

C Ablation studies

In the proposed m2mKD pipeline, the stitch layers are used only during the distillation phase and subsequently discarded to ensure no modifications are required for the student model. Although the stitch layers typically account for just a small proportion of the total parameters in a large modular model (e.g., 1% for our V-MoE-B student), directly removing them may result in the loss of some knowledge acquired from the teacher, potentially impacting the final model’s performance negatively. To investigate this, we conduct experiments preserving the stitch layers in the student model. However, as shown in Table 11, the results indicate no noticeable improvement from this approach. Consequently, we maintain our decision to discard the stitch layers.

Some additional experiments are conducted based on the setting of preserving stitch layers. The previous experiment indicates that the presence of the stitch layers does not influence much, so we suppose the following conclusions are applicable regardless of their removal. Firstly, since the NAC models are able to achieve great improvement with student modules distilled for merely 10 epochs, we test the performance of V-MoE-B models under the same condition. To this end, we adjust some of the hyperparameters of the m2mKD phase and distill the student module for 10 epochs. The E2E phase remains to be 100 epochs. Table 11 shows that decreasing the distillation epochs from 100 to 10, the accuracy drops 2.1%, but is still 2.8% better than the Deep Incubation baseline. We apply the same changes on the incubation phase of Deep Incubation and, surprisingly, there is no degradation of the performance using the new hyperparameters. Next, we inspect the scalability of m2mKD. The DeiT-Huge model (632M) pretrained by Deep Incubation is chosen as the teacher. The student model ($L = 4$) is a V-MoE-Large model with 12 MoE layers placed on every other layer, which totally contains 1.0B parameters. Table 11 compares m2mKD with Deep Incubation and the former achieves 0.27% higher accuracy on ImageNet-1k.

The remaining ablation experiments are conducted based on the preservation of stitch layers. The previous experiment indicates that the presence of the stitch layers does not have a significant influence, we believe that

Table 11: **Results of ablation studies.** The hyperparameters adjusted for decreasing distillation epochs are as follows: warm-up-epochs=5, warm-up-lr=0.0001, min-lr=0.002. The ratio of training time is calculated relative to the time used in the pure end-to-end training approach. The column for V-MoE-L is empty because we did not train our V-MoE-L model using the pure end-to-end method. Note that all experiments, except the *baseline*, are conducted with stitch layers inserted in the student model.

		Acc@1	Acc@5	Extra params	Ratio of Time
m2mKD	baseline	81.90	95.43	0	0.99
	w/ stitch	81.93	95.53	4.7M (1%)	0.99
	10 epochs	81.72	95.44	0	0.57
Deep Incubation	baseline	81.40	95.06	0	0.91
	10 epochs	81.44	95.09	0	0.54
V-MoE-L	m2mKD	83.36	96.42	7.9M (0.8%)	N/A
	Deep Incubation	83.09	96.12	0	N/A

the following conclusions remain valid regardless of their removal. Firstly, since the NAC models demonstrate considerable improvement with student modules distilled for only 10 epochs, we test the performance of V-MoE-B models under the same condition. To this end, we adjust some of the hyperparameters during the m2mKD phase and distill the student module for 10 epochs, while retaining the E2E phase at 100 epochs. As shown in Table 11, decreasing the distillation epochs from 100 to 10 results in a drop of 2.1% in accuracy, yet it remains 2.8% higher than the Deep Incubation baseline. Surprisingly, applying the same changes to the incubation phase of Deep Incubation does not lead to any performance degradation. Next, we examine the scalability of m2mKD. The teacher model is the DeiT-Huge model (632M) pretrained by Deep Incubation, while the student model ($L = 4$) is a V-MoE-Large model with 12 MoE layers placed on every other layer, resulting in a total of 1.0B parameters. As presented in Table 11, m2mKD outperforms Deep Incubation by 0.27% in terms of accuracy on ImageNet-1k.